

Electronic structure of Ge/Si quantum dots

A V Dvurechenskii¹, A V Nenashev² and A I Yakimov¹

¹ Institute of Semiconductor Physics, Siberian Branch of the Russian Academy of Sciences, 630090 Novosibirsk, Russia

² Novosibirsk State University, 630090 Novosibirsk, Russia

E-mail: dvurech@isp.nsc.ru

Received 12 September 2001, in final form 24 October 2001

Published xx Month 2002

Online at stacks.iop.org/Nano/13/S1

Abstract

We have investigated theoretically the strain distribution in pyramid-shaped Ge/Si quantum dots (QDs) and their environment, using the atomistic approach and Green function technique. Taking into account the results of strain calculations, we have studied the hole discrete spectrum by the tight-binding method. Energy levels, their dependence on dot size and wavefunction density distributions have been obtained. We have proposed a method for calculation of the Landé factor for localized states in QDs and calculated the value of the g -factor for the ground state in the Ge/Si dot. We have developed the theoretical model of spatially indirect excitons and excitonic complexes, localized on the QD. The binding energy and optical transition energy have been calculated for excitonic complexes with different numbers of electrons and holes.

Ascii/Word/NAN/na128738/SPE
Printed 4/1/2002

Issue no
Total pages
First page
Last page
File name NA .TEX
Date req
(S)

1. Introduction

The determination of the energy spectrum, kinetics of transitions between electronic levels and interactions of elementary excitations, as well as correlation effects, form a base of current fundamental studies of quantum dots (QDs). Recent results of optical and electrical investigations of QDs fabricated on the base of Ge/Si [1] demonstrated that these structures have unique potential for applications in nano- and opto- electronics. The physical properties of this system depend on parameters of the QD (size, shape, lattice mismatch), and the modelling of physical objects became a powerful method for understanding real experiment results and for predictions of new ones. Ge/Si(001) QDs exhibit a type-II band lineup. The large (~ 0.7 eV) valence band (VB) offset in this heterojunction leads to effective localization of holes in the Ge regions, whereas these Ge regions represent potential barriers for electrons. When the hole is captured by the Ge dot, its Coulomb potential results in binding of an electron in the vicinity of the Ge dot. The spatially separated interacting electron and hole are usually referred to as a spatially indirect exciton.

There are many papers devoted to electronic structure calculation in self-assembled QDs, using the effective mass approximation [2–6], pseudopotentials [7] and the tight-binding (TB) approach [8], but these studies concentrate

mainly on the InAs/GaAs heterosystem. Regarding Ge QDs, realistic calculations of energy spectrum have been performed only for free-standing spherical Ge nanoclusters [9]. To our knowledge, there are no energy spectrum calculations for pyramid-shaped self-assembled Ge islands. Also theoretical studies of the g -factor [10] and properties of indirect excitons [11, 12] in self-assembled QDs were only performed for the model case of a spherical dot.

The aim of this work is computer modelling of electronic structures of Ge/Si QDs and numerical investigation of properties of spatially indirect excitons.

2. Strain distribution

The elastic strain due to the lattice mismatch between islands and the surrounding matrix has essential effects on the electronic structure of QDs [2, 13]. Sizes of the studied islands are too small for consideration of their elastic properties in terms of the continuum approach. In the present paper strain distribution has been found in the atomistic approach, in terms of atomic positions, using Keating's valence-force-field model [14].

The calculation was based on an original Green function method [13], which allows us to reduce considerably the computation resources. Conventional strain calculation

techniques suppose periodic boundary conditions, and a large calculation domain (or ‘supercell’) is needed to reduce the unphysical elastic dot–dot interaction [7]. In contrast to this, the Green function technique is not sensitive to the size of calculation domain, and this allows us to shrink the calculation domain so that only the atoms of the island and its immediate surroundings are involved in the strain calculation.

Typical pyramidal Ge/Si islands with four {105}-oriented facets and a (001) base, lying on a wetting layer of 0.7 nm thickness, have been under study. The island size (the length of the base side) has been varied from 6 to 15 nm. Ge islands and wetting layer are embedded into the Si matrix.

The spatial distribution of strain in the Ge/Si QD has been obtained. Inside the island the largest stress arises on the periphery of the pyramid base, and the greatest relaxation occurs in the apex of the pyramid, whereas the vicinity of the pyramid apex in Si is most stressed over the Si matrix. The main characteristic of the strain tensor is the compression in the lateral plane and the dilatation in the growth direction throughout the Ge island.

The analysis of the size dependence of the strain shows the following results:

(a) values of strain components $\varepsilon_{\alpha\beta}$ are independent of the dot size over the range of size 10–15 nm in the central region of the dot; this means that the macroscopic value of the strain tensor is already reached in this range;

(b) components of the strain tensor increase in absolute value logarithmically with QD size near the edge of the pyramid base. This is in agreement with the macroscopic behaviour.

The obtained spatial strain distribution was involved in the calculation of the hole energy spectrum and energies of excitonic transitions of Ge QDs.

3. Hole energy spectrum

The energy spectrum was obtained by means of the sp^3 TB approach, including interactions between nearest neighbours only [15, 16]. Following the work of Chadi [17], spin-orbit interactions were added to the Hamiltonian. Strain effects are incorporated into the Hamiltonian in two ways: as changes of interatomic matrix elements and as the strain-induced mixing of orbitals centred on the same atom. The changes of interatomic matrix elements due to strain are treated by the generalization of Harrison’s d^{-2} law [18],

$$ijk(d) = ijk(d_0) \left(\frac{d_0}{d} \right)^{n_{ijk}},$$

for bond length d and by the Slater and Koster formulae [15] for bond angles. There ijk are two-centre integrals, d_0 is the unstrained bond length and n_{ijk} are orbital-dependent exponents reflecting the localization of the atomic wavefunctions near the nuclei. For description of the strain influence on mixing of p orbitals we include in the TB Hamiltonian the matrix elements between p orbitals belonging to the same atom:

$$\begin{aligned} \langle p_x | \hat{H} | p_y \rangle &= -\beta \varepsilon_{xy}, & \langle p_x | \hat{H} | p_z \rangle &= -\beta \varepsilon_{xz}, \\ \langle p_y | \hat{H} | p_z \rangle &= -\beta \varepsilon_{yz}, \end{aligned} \quad (1)$$

Table 1. TB parameters for Si and Ge. E_s and E_p are on-site Hamiltonian matrix elements, $ss\sigma \dots pp\pi$ are two-centre integrals [15], Δ is the spin-orbit coupling energy, $n_{ss\sigma} \dots n_{pp\pi}$ are orbital-dependent exponents reflecting the localization of the atomic wavefunctions near the nuclei [18] and β is the parameter that appears in equation (1).

Parameter	Si	Ge
E_s (eV)	−0.51	−3.32 + 0.55
E_p (eV)	0.70	0.89 + 0.55
$ss\sigma$ (eV)	−1.03	−1.03
$sp\sigma$ (eV)	3.01	3.00
$pp\sigma$ (eV)	1.755	2.42
$pp\pi$ (eV)	−0.61	−0.84
Δ (eV)	0.04	0.29
$n_{ss\sigma}$	2.00	2.00
$n_{sp\sigma}$	2.00	2.00
$n_{pp\sigma}$	2.00	1.78
$n_{pp\pi}$	1.37	2.00
β (eV)	5.63	5.89

where ε is the strain tensor and β is the model parameter.

The mixing of orbitals introduced by equation (1) allows us to fit the value of shear deformation potential d . Another deformation potential, b , can be varied in a similar way by taking into account the influence of diagonal strain components on energies of orbitals [18]. We however do not include this effect in our model, because it is not necessary for reproducing the correct value of the deformation potential b .

Values of parameters are presented in table 1. They are chosen to fit values of heavy-hole and light-hole effective masses and VB deformation potentials. We include in E_s and E_p the VB offset between non-strained Si and Ge, which is equal to 0.55 eV. All parameters for Si–Ge bonds are taken as arithmetic means between Si and Ge parameters.

Finding eigenvalues of the Hamiltonian \hat{H} is performed by a method analogous to that of Pedersen and Chang [19]. These authors solved the equation

$$\frac{\partial}{\partial \tau} |\psi(\tau)\rangle = -\hat{H} |\psi(\tau)\rangle,$$

where τ is imaginary time parameter: $\tau = it$. When $\tau \rightarrow \infty$ the solution $|\psi(\tau)\rangle$ will relax towards the lowest-energy state. Because we are interested in energy values within the bandgap, we have modified the method following the idea of Wang and Zunger [20]. We fixed the reference energy value E_{ref} lying in the bandgap, then we solved the equation

$$\frac{\partial}{\partial \tau} |\psi(\tau)\rangle = -(\hat{H} - E_{\text{ref}}) |\psi(\tau)\rangle. \quad (2)$$

In the limit $\tau \rightarrow \infty$ the equation (2) gives an eigenstate of \hat{H} corresponding to an energy level nearest to E_{ref} . Then the value of energy E can be found as $E = \langle \psi(\tau) | \hat{H} | \psi(\tau) \rangle / \langle \psi(\tau) | \psi(\tau) \rangle |_{\tau \rightarrow \infty}$.

The geometry and symmetry of problem in itself provides some conclusions about energy spectrum. The geometry of the island results in a strong difference between the values of size quantization energy in the plane of the pyramidal base and in the growth direction. The difference between ground state and some number of excited states therefore has to be determined only by quantization in the base plane. The degeneracy of energy levels is defined by twofold representations of the

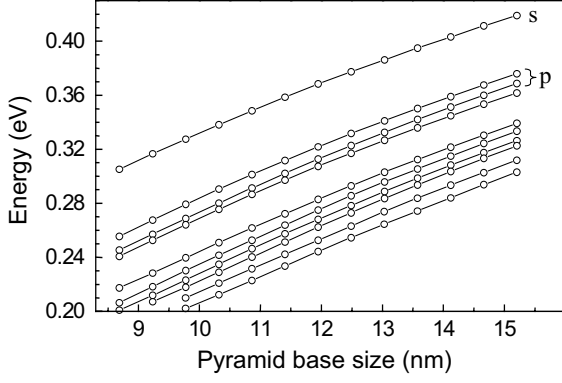


Figure 1. Energy spectrum of holes in the pyramidal Ge/Si QD as a function of pyramid base size. The energy is counted from the VB edge in bulk Si. The ground state (upper curve) and nine excited states are shown. Characters s and p indicate s-like (ground) and p-like states, correspondingly.

symmetry group C_{2v} , therefore all the levels are twofold degenerate. The symmetry of the problem is similar to a disc symmetry, that allows us to make the assumption that the ground state will be s-like and the next two states will be p-like.

Calculated energies of the ground state and the next nine excited states of the hole spectrum are presented in figure 1 as a function of island size. Separations between levels remain practically unchangeable for all sizes in the region 8–15 nm. The found wavefunctions are characterized by absence of nodal surfaces perpendicular to the growth direction. From the distribution of charge density (figure 2) we conclude that the ground state has an s-like wavefunction, and the first two excited states have p-like wavefunctions oriented along $[110]$ and $[\bar{1}10]$. The next excited states have more complicated wavefunction structure. The splitting between two p-like states is about 7 meV, and it is caused by two factors: spin-orbit interaction and nonequivalence of directions $[110]$ and $[\bar{1}10]$ in the case of an atomically sharp Ge/Si(100) interface. To separate contributions of these effects to the splitting of the p-levels, we solved the problem with a diffused interface on the base of the pyramid, in which the last monolayer of Si under the Ge island contains 33% Ge, and the first Ge monolayer in the base of the island contains 33% Si. In the case of a diffused Ge/Si interface, p-like states have no preferred orientation, and splitting between them decreases until ~ 3 meV. This remaining splitting arises from the spin-orbit interaction.

The absence of nodal surfaces perpendicular to the growth direction is clear evidence that the difference between all the found states is determined only by quantization in the plane of pyramid base. Therefore optical transitions between these states must be stimulated by irradiation polarized in the base plane, that agrees with experimental results [21, 22]. The weak size dependence of separations between levels allow to conclude that optical transition lines in the QD array will be well resolved even if there is a dispersion of QD sizes within the investigated range of size.

4. g -factor of holes

Based on the TB approach we developed a method for calculation of the g -factor of localized states. This method

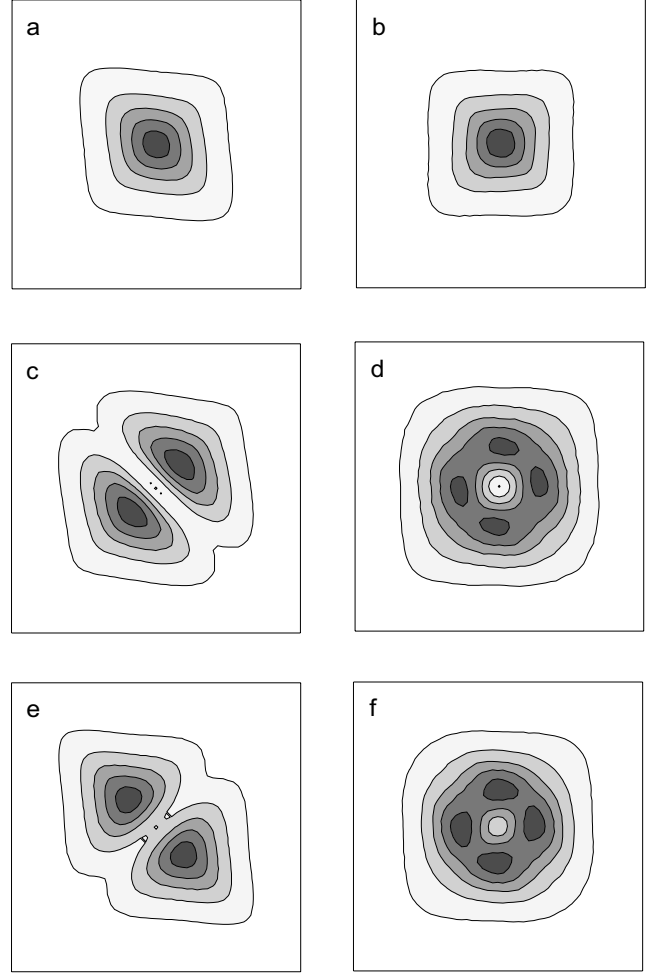


Figure 2. Probability density isosurfaces of (a), (b) ground state, (c), (d) first excited state and (e), (f) second excited state of a hole in the Ge/Si QD. Left part (a), (c), (e) is related to the case of sharp interfaces, right part (b), (d), (f) is related to the case of a diffuse interface on the base of the pyramid. Projections on the plane perpendicular to the growth direction are shown. Edges of the pyramidal Ge island are denoted by squares.

is applicable when the size of the wavefunction is comparable to the interatomic distance.

External magnetic field removes the twofold Kramers degeneration of localized states in the QD. Generally, in small fields this splitting can be written as $\Delta E = \mu_B g H$, where μ_B is the Bohr magneton, H is the magnetic field and g is an effective g -factor of the state. In the case when ΔE is small in comparison with size quantization energies, the g -factor depends only on the magnetic field direction, and can be evaluated by means of the first-order perturbation theory:

$$|g| = 2(\langle \psi | \mathbf{n}(\hat{\mathbf{L}} + \hat{\boldsymbol{\sigma}}) | \psi \rangle^2 + |\langle \psi | \mathbf{n}(\hat{\mathbf{L}} + \hat{\boldsymbol{\sigma}}) | \varphi \rangle|^2)^{1/2}. \quad (3)$$

There $\{|\psi\rangle, |\varphi\rangle\}$ is the Kramers doublet of states of some energy level; \mathbf{n} is the unit vector in the magnetic field direction; $\hat{\mathbf{L}}$ is the orbital angular momentum operator and $\hat{\boldsymbol{\sigma}}$ is the vector of Pauli matrices.

Vectors $|\psi\rangle, |\varphi\rangle$ can be obtained as linear combinations of atomic orbitals by solving the eigenvalue problem, as described above. Thus, to calculate matrix elements contributing to (3), one has to determine how the operator $\hat{\mathbf{L}}$ acts on atomic orbitals. In other words, one should find the expression for $\hat{\mathbf{L}}$ in the representation of atomic orbitals.

The angular momentum depends on the choice of the origin of the coordinate system. Let $\hat{L}(X^0, Y^0, Z^0)$ be an orbital angular momentum operator in a coordinate system with origin at the $\mathbf{R}^0 = (X^0, Y^0, Z^0)$ point. Then,

$$\hat{L}_\alpha \equiv \hat{L}_\alpha(0, 0, 0) = \hat{L}_\alpha(X^0, Y^0, Z^0) + \frac{1}{\hbar} e_{\alpha\beta\gamma} R_\beta^0 \hat{p}_\gamma, \quad (4)$$

where \hat{p} is the momentum operator, $e_{\alpha\beta\gamma}$ is the unit antisymmetric tensor; indices α, β, γ run over the set $\{x, y, z\}$.

Let $|a, b\rangle$ denotes an orbital, where a is the number of the atom on which this orbital is centred and b is the type of orbital; b takes values from the set $\{s, p_x, p_y, p_z\}$. We introduce two operators: the operator $\hat{R} = (\hat{X}, \hat{Y}, \hat{Z})$, which acts on atomic orbitals as

$$\hat{R}|a, b\rangle = \mathbf{R}_a|a, b\rangle,$$

where $\mathbf{R}_a = (X_a, Y_a, Z_a)$ denotes the position of atom a , and the operator $\hat{L}^{(0)}$, which acts according to the rule

$$\hat{L}^{(0)}|a, b\rangle = \hat{L}(X_a, Y_a, Z_a)|a, b\rangle.$$

We can now rewrite equation (4), assuming that $\mathbf{R}^0 = \mathbf{R}_a$, in the form of

$$\hat{L}_\alpha = \hat{L}_\alpha^{(0)} + \frac{1}{\hbar} e_{\alpha\beta\gamma} \hat{p}_\gamma \hat{R}_\beta. \quad (5)$$

The result of the action of operator $\hat{L}^{(0)}$ on the orbital $|a, b\rangle$ depends only on the orbital type, not on the position of atom a . Neglecting the distortion of orbitals caused by the interaction with neighbouring atoms, we have for any atom a

$$\hat{L}^{(0)}|a, s\rangle = 0, \quad (6a)$$

$$\hat{L}_\alpha^{(0)}|a, p_\beta\rangle = i e_{\alpha\beta\gamma} |a, p_\gamma\rangle. \quad (6b)$$

The momentum operator \hat{p} can be expressed through the co-ordinate operator \hat{r} by the formula

$$\hat{p} = \frac{im}{\hbar} (\hat{H}_0 \hat{r} - \hat{r} \hat{H}_0), \quad (7)$$

where m is the mass of the free electron and $\hat{H}_0 = \hat{H} - \hat{H}_{so}$ is the full Hamiltonian \hat{H} minus the term \hat{H}_{so} responsible for the spin-orbit interaction. Equation (7) can be deduced from the expression $\hat{H}_0 = \hat{p}^2/2m + U(\mathbf{r})$ or from the time differentiation rule for operators [23]. Further we assume that the operator \hat{r} can replace the operator \hat{R} in equation (7), since the difference $\hat{r} - \hat{R}$ does not exceed the atomic radius. Making this replacement and substituting equation (7) into equation (5), one can find the compact form for the orbital angular momentum operator:

$$\hat{L}_\alpha = \hat{L}_\alpha^{(0)} + \frac{im}{\hbar^2} e_{\alpha\beta\gamma} \hat{R}_\beta \hat{H}_0 \hat{R}_\gamma. \quad (8)$$

For example, for the z -component this gives

$$\hat{L}_z = \hat{L}_z^{(0)} + \frac{im}{\hbar^2} (\hat{X} \hat{H}_0 \hat{Y} - \hat{Y} \hat{H}_0 \hat{X}).$$

So, if one knows the Hamiltonian \hat{H} and its eigenvalues $|\psi\rangle$ and $|\varphi\rangle$ in terms of atomic orbitals, then one can calculate the g -factor using equations (3), (8) and (6).

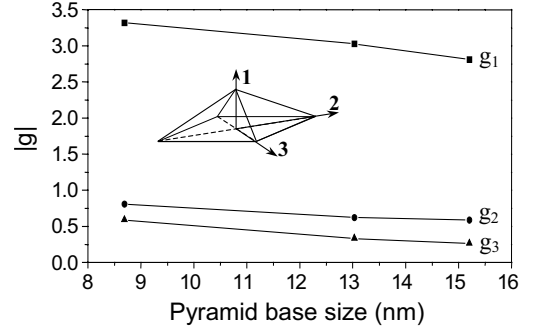


Figure 3. Dependence of g -factor principal values of ground hole state in the Ge/Si QD on the dot size. The inset shows the principal directions of the g -tensor.

In the frame of the developed approach, we calculated the g -factor for the ground hole state in the Ge/Si QD. We found the principal values of g -tensor for directions $[001]$ (the growth direction), $[110]$ and $[\bar{1}10]$, and in the case of the QD with 15 nm size these values are $|g_1| = 2.81$, $|g_2| = 0.59$ and $|g_3| = 0.26$, correspondingly. When the size of dot is decreased to 9 nm, the main values $|g_1|$, $|g_2|$ and $|g_3|$ are increased to 3.32, 0.81 and 0.59, correspondingly (figure 3).

5. Energetic structure of excitons and excitonic complexes

To obtain the binding energy of the excitonic complexes consisting of various numbers of electrons and holes captured on the Ge/Si QD, we developed a mathematical model of the excitonic complex based on the effective-mass approximation. The realistic geometry of the Ge island is included in the model. The length of the pyramid base is assumed to be equal to 15 nm. Since we consider only the ground state of the excitonic complex, we restrict the model by consideration of only the lowest minimum of the conduction band (CB) and the highest VB maximum. From the strain distribution [13] and deformation potential values [24] it was found that two Δ valleys, oriented along the growth direction, offer the lowest CB minimum in Si. The heavy-hole branch produced the highest VB maximum in the Ge island. The confining potential for electrons and holes consists of the band offset between unstrained Si and Ge and strain-induced modification of conduction and valence bands. We use the band offset values of 0.34 eV for the Δ minimum of the CB and 0.61 eV for the VB. Values of deformation potentials are taken from [15]. Effective masses of both electrons and holes are taken to be anisotropic, and is assumed for simplicity that masses are co-ordinate independent. Let m_z and m_{xy} be effective masses in the growth direction and in the plane orthogonal to it, correspondingly. We use values of longitudinal and transversal effective masses of the Δ minimum in Si as m_z and m_{xy} , correspondingly; so $m_z = 0.92m_0$ and $m_{xy} = 0.19m_0$ for the CB. In the VB, we use values $m_z = 0.2m_0$ (the heavy-hole mass in Ge in the $\langle 001 \rangle$ directions) and $m_{xy} = 0.39m_0$. The value of m_{xy} for the VB is taken so as to make the value of averaged effective mass $m_{av} = m_{xy}^{2/3} m_z^{1/3}$ coincide with the averaged heavy-hole mass in Ge. The interaction between charged particles is taken in the form of the Coulomb potential $U(\mathbf{r}_i, \mathbf{r}_j) = q_i q_j / 4\pi \epsilon_0 |\mathbf{r}_i - \mathbf{r}_j|$. We assume the

value $\varepsilon = 11.9$ (the dielectric constant of Si) for electron–electron and electron–hole interactions, and the value $\varepsilon = 16$ (the dielectric constant of Ge) for hole–hole interactions.

To solve the many-particle problem, the Hartree approximation is used; i.e., a separable exciton wavefunction is assumed and the single electron and hole states are determined self-consistently. The set of Schrödinger equations was solved by the finite-difference method using the grid with period of **0.543 nm** (the lattice constant of Si) containing $50 \times 50 \times 60$ nodes. To reduce an error that arises from the finite size of the grid, the calculation was performed twice with different boundary conditions applied: once with Dirichlet boundary conditions ($\psi|_{\text{boundary}} = 0$), that gives an upper estimate for energy levels, and with Neumann boundary conditions ($\partial\psi/\partial n|_{\text{boundary}} = 0$), that gives a lower estimate. The arithmetic mean of the two estimates is taken as a final result. According to the Pauli principle, filling of each VB level with only two holes and of each CB level with only four electrons was permitted. Four electrons can occupy the same CB level, because there are two equivalent Δ valleys and two equivalent spin states.

Energies of interband optical transitions corresponding to adding an exciton to the Ge/Si QD was calculated. We denote the energy of transition from the empty dot state to the state with one electron and one hole in the QD as $E_{0e0h \rightarrow 1e1h}$, and so on. Calculated values are $E_{0e0h \rightarrow 1e1h} = 629.6$ meV, $E_{0e1h \rightarrow 1e2h} = 639.3$ meV, $E_{1e1h \rightarrow 2e2h} = 639.8$ meV. Therefore one excess hole in the dot causes an increase of the excitonic transition energy by 9.7 meV. This blueshift of the excitonic line is a consequence of the spatial separation of electrons and holes, which is a characteristic of type-II QDs. Indeed, neglecting for simplicity the perturbation of electron and hole wavefunctions by the second hole in the dot, we have

$$E_{0e1h \rightarrow 1e2h} = E_{0e0h \rightarrow 1e1h} + V_{eh} + V_{hh},$$

where V_{eh} and V_{hh} are electron–hole and hole–hole interaction energies. Since the mean distance between electron and hole is larger than between two holes, then $|V_{eh}| < |V_{hh}|$. Therefore $E_{0e1h \rightarrow 1e2h} > E_{0e0h \rightarrow 1e1h}$.

We found that in the case of an exciton consisting of one electron and one hole, the hole is located in the centre of the pyramidal Ge island, and the electron is confined in the Si vicinity of the island apex [25, 26]. This location of the electron is due to, firstly, inhomogeneous strain which forms the confining potential for electrons near the apex of the pyramid and, secondly, the Coulomb attraction to the hole. When a new electron is added to the QD, it is found to be spatially separated from the first one and located under the base of the pyramid symmetrically to the first electron [26, 27]. At further filling of the dot the third electron added to the apex well, the fourth to the based well and so on.

The energy of excitonic transition in the QD already containing an exciton, $E_{1e1h \rightarrow 2e2h}$, is larger by 10.2 meV as compared with $E_{0e0h \rightarrow 1e1h}$, the excitonic transition energy in the empty QD. This follows from the fact that the second electron in the excitonic complex is localized in a shallower potential well than the first one.

The results of calculations have been verified experimentally [25, 26]. In the experiment, interband absorption in the

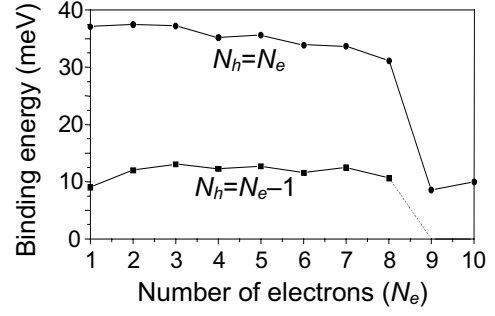


Figure 4. Binding energy of electron trapped by the Ge/Si QD, as a function of numbers of electrons (N_e) and holes (N_h) bound on the dot. The upper curve was calculated for a neutral QD ($N_h = N_e$) and the bottom curve for a negatively single-charged QD ($N_h = N_e - 1$).

QD array was studied by electron-filling modulation spectroscopy. The p^+-p-n^+ structure with a QD array embedded into the p layer was used. The number of holes in the QDs can be tuned by an external applied bias. To create excitons localized on QDs, interband optical pumping was used. Shifts of the excitonic transition line, caused by changing population of holes or excitons in the QDs, are found in satisfying agreement with calculation results.

We also have calculated the electron binding energy, i.e. the energy needed to move an electron to infinity, in the excitonic complex containing different numbers of electrons (N_e) and holes (N_h). Calculations show that, for $N_h < 8$, QD can keep $N_h + 1$ electrons. A shallow bound electron state exists even when no holes are in the dot ($N_h = 0$, $N_e = 1$). This is due to nonuniform strain of the silicon matrix. Addition of one electron and one hole to the QD gives rise to an increase of binding energy, because in this case ($N_h = 1$, $N_e = 2$) the extra electron and hole form a dipole which creates an additional attractive potential. When N_h increases, the binding energy of the $N_h + 1$ th electron increases up to $N_h = 2$, and then slightly decreases (figure 4). For $N_h = 8$, the ninth electron cannot be captured by the QD, since each electronic potential well (above and below the Ge island) has one fourfold degenerate quantum level, and both these levels are fully occupied by eight electrons. In the case when $N_e = N_h$ (the upper curve in figure 4) potential wells for electrons are deeper than for the case $N_e = N_h + 1$ (the lower curve), therefore the dot with nine holes can trap the ninth electron.

The dependence of electron binding energy on the number of electrons and holes provides an explanation for the negative photoconductivity observed recently in the n-type Ge/Si QD structure [28, 29]. QDs serve as traps for free electrons. When electron–hole pairs are photogenerated, nonequilibrium holes and electrons are captured by QDs. As a result, the depth of traps for electrons (or the electron binding energy) increased with increasing number of electrons and holes (figure 4, lower curve) and therefore additional equilibrium electrons are trapped. Thus the concentration of free electrons decreases with illumination, and conductivity falls. The negative photoeffect is one of the effects characteristic only for type-II QDs.

6. Summary

In this work we have touched on four subjects of QD studies: (1) strain distribution; (2) energy spectrum; (3) g -factor; (4) excitonic properties.

First, we developed a new approach for calculation of strain distribution in QDs and their environment using the Keating atomic potential and Green function technique. This approach was applied to the pyramid-shaped Ge/Si QD.

Second, the hole discrete spectrum in Ge/Si QD were studied by the TB method. Energy levels, its dependence on dot size and wavefunction density distributions were obtained. Distances between levels were found to be practically unchangeable for all sizes in the region 8–15 nm. We concluded that the optical transitions between localized states must be stimulated by irradiation polarized in the base plane. This was in agreement with experimental results.

Third, we proposed a method for calculation of the Landé factor for localized states in QDs. Values of g -factor for the ground state in Ge/Si dots had been found. The principal values of g -tensor for the case of a QD with 15 nm size are $|g_1| = 2.81$, $|g_2| = 0.59$ and $|g_3| = 0.26$, and they increase with decreasing QD size.

Fourth, the model of spatially indirect excitons and excitonic complexes, localized on the Ge QD, was formulated. We calculated the binding energy and optical transition energy for excitonic complexes for different numbers of electrons and holes. Calculations shown that, for number of holes $N_h < 8$, the QD can keep $N_h + 1$ electrons. When N_h increases, the binding energy of the $N_h + 1$ th electron increases up to $N_h = 2$, and then slightly decreases. The obtained results allow us to understand the negative photoconductivity observed recently in the n-type Ge/Si QD structure. Also, the spatial structure was determined for single and double excitons on the Ge/Si QD.

Acknowledgments

We gratefully acknowledge Dr N P Stepina for regular interest in the work and fruitful discussions. This work was supported by Russian programmes ‘Physics of solid state nanostructures’ (grant 98-1100, 00-17-2F), Education Ministry programme (grant E00-3.4-154), Russian Foundation of Basic Research and the Natural Science National Fund of China (grant 99-02-39051) and RFBR (grant 00-02-17885).

References

- [1] Dvurechenskii A V and Yakimov A I 1999 *Izv. Vyssh. Uchebn. Zaved, Mater. Electron.* No 4 4
Dvurechenskii A V, Yakimov A I, Markov V A, Nikiforov A I and Pchelyakov O P 1999 *Izv. Akad. Nauk Fiz.* **63** 307
- Dvurechenskii A V and Yakimov A I 2000 *Izv. Akad. Nauk Fiz.* **65** 306
- Pchelyakov O P, Bolkhovitanov Yu B, Dvurechenskii A V, Sokolov L V, Nikiforov A I, Yakimov A I and Voigtländer B 2000 *Semiconductors* **34** 1281
- Dvurechenskii A V and Yakimov A I 2001 *Izv. Akad. Nauk Fiz.* **65** 187
- [2] Grundmann M, Stier O and Bimberg D 1995 *Phys. Rev. B* **52** 11 969
- [3] Cusack M A, Briddon P R and Jaros M 1997 *Phys. Rev. B* **56** 4047
- [4] Jiang H and Singh J 1997 *Phys. Rev. B* **56** 4696
- [5] Pryor C 1998 *Phys. Rev. B* **57** 7190
- [6] Stier O, Grundmann M and Bimberg D 1999 *Phys. Rev. B* **59** 5688
- [7] Wang L-W, Kim J and Zunger A 1999 *Phys. Rev. B* **59** 5678
- [8] Saito T, Schulman J N and Arakawa Y 1998 *Phys. Rev. B* **57** 13 016
- [9] Niquet Y M, Allan G, Delerue C and Lannoo M 2000 *Appl. Phys. Lett.* **77** 1182
- [10] Kiselev A A and Ivchenko E L 1998 *Phys. Rev. B* **58** 16 353
- [11] Takagahara T and Kyozauro T 1992 *Phys. Rev. B* **46** 15 578
- [12] Rorison J M 1993 *Phys. Rev. B* **48** 4643
- [13] Nenashev A V and Dvurechenskii A V 2000 *Zh. Eksp. Teor. Fiz.* **118** 570 (Engl. transl. *JETP* **91** 497)
- [14] Keating P N 1966 *Phys. Rev.* **145** 637
- [15] Slater J C and Koster G F 1954 *Phys. Rev.* **94** 1498
- [16] Chadi D J and Cohen M L 1975 *Phys. Status Solidi b* **68** 405
- [17] Chadi D J 1977 *Phys. Rev. B* **16** 790
- [18] Jancu J-M, Scholz R, Beltram F and Bassani F 1998 *Phys. Rev. B* **57** 6493
- [19] Pedersen F B and Chang Y-C 1996 *Phys. Rev. B* **53** 1507
- [20] Wang L-W and Zunger A 1994 *J. Chem. Phys.* **100** 2394
- [21] Yakimov A I, Dvurechenskii A V, Proskuryakov Yu Yu, Nikiforov A I, Pchelyakov O P, Teys S A and Gutakovskii A K 1999 *Appl. Phys. Lett.* **75** 1413
- [22] Yakimov A I, Dvurechenskii A V, Stepina N P and Nikiforov A I 2000 *Phys. Rev. B* **62** 9939
- [23] Landau L D and Lifshits E M 1989 *Quantum Mechanics* (Moscow: Nauka)
- [24] Van de Walle C G 1989 *Phys. Rev. B* **39** 1871
- [25] Yakimov A I, Stepina N P, Dvurechenskii A V, Nikiforov A I and Nenashev A V 2000 *Semicond. Sci. Technol.* **15** 1125
- [26] Yakimov A I, Dvurechenskii A V, Stepina N P, Nikiforov A I and Nenashev A V 2001 *Zh. Eksp. Teor. Fiz.* **119** 574 (Engl. transl. *JETP* **92** 500)
- [27] Yakimov A I, Stepina N P, Dvurechenskii A V, Nikiforov A I and Nenashev A V 2001 *Phys. Rev. B* **63** 045312
- [28] Yakimov A I, Dvurechenskii A V, Nikiforov A I, Pchelyakov O P and Nenashev A V 2000 *Phys. Rev. B* **62** 16 283
- [29] Yakimov A I, Dvurechenskii A V, Nikiforov A I and Pchelyakov O P 2000 *Pis'ma Zh. Eksp. Teor. Fiz.* **72** 267 (Engl. transl. *JETP Lett.* **72** 186)

Queries for IOP paper 128738

Journal: **Nano**

Author: **A V Dvurechenskii et al**

Short title: **Electronic structure of Ge/Si quantum dots**

Page 5

Query 1:

Author: Please check the unit 'nm' OK?